The 2010 IEEE/RSJ International Conference on
Intelligent Robots and Systems
October 18-22, 2010, Taipei, Taiwan

Path Planning of a Mobile Robot for Avoiding Moving Obstacles with Improved Velocity Control by Using the Hydrodynamic Potential

Seiji Sugiyama, Jyun Yamada and Tsuneo Yoshikawa

Abstract— **This paper describes the theory and the simulation of an improved velocity potential approach for path planning by which a mobile robot avoids standing and/or moving obstacles by using the hydrodynamic potential. This potential function for path planning is feasible for guiding a mobile robot to avoid an arbitrarily moving obstacle and to reach the goal in real time without finding the local maximum or minimum points in all cases. In this theory, there are two problems. One is that a mobile robot accelerates rapidly when it avoids a moving obstacle. The other is that a mobile robot has a discontinuous velocity when it is passing a moving obstacle. An ellipse field, which is obtained by using the conformal transformation, and a correction function, which generates the continuous velocity field, are installed in the previous potential function to cope with the difficulty. As a result, a mobile robot can gradually avoid a moving obstacle from further away, and can be safely guided without rapid acceleration.**

I. INTRODUCTION

Autonomous robots are demanded extensively in many fields for reducing the work quantity of humans and giving us a comfortable life. Especially, the expectation of moving robots in a real environment is too much, so mobile robots should be constructed. However, there are few such mobile robots for use in daily life, because existing mobile robots are only moving in a limited environment and/or the humans must keep watching the robots. One of the bottlenecks is the relation between the robot and humans who are arbitrarily moving around the robot when the robot is running in a real environment. That is, a mobile robot should avoid such moving humans and/or obstacles.

There have been two main streams in solving the problem of path planning. One is Artificial Intelligence (AI). When only ambiguous geometry of the environment is available to the robot, AI approach is useful. The other is Artificial Potential approach. When perfect geometric information of the environment is available, the physical field approach is more attractive than AI approach because of its high efficiency in path planning [1][2]. Recently, the performances of sensors are getting well. Therefore, we assume that the environment information is already given in this research.

Artificial Potential functions have been proposed and investigated since Khatib [3]. In these theories, the effect of a goal is represented by attractive potential, and that of the obstacles or the boundary is represented by repulsive potential. A mobile robot applies the force generated by artificial potentials as control inputs to the driving system. Khatib's potential has a stagnation point due to the effects of a interference between the obstacle and the goal. Khosla has proposed a solution to the problem by using the potential satisfying the Laplace equation [4]. If it satisfies the Laplace equation, a mobile robot can reach the goal without finding the local maximum or minimum point in all cases.

The usefulness of this theory can be understood easily by supposing the following situation. A shallow vessel is filled with water. A body with a closed boundary can be introduced inside the vessel. This body may move itself. When the drain point in the vessel is opened, the flow is generated. A particle in the water moves toward the drain point smoothly from any location (Fig. 1). A mobile robot is controlled by using the same dynamics as the flow of the water. A two-dimensional flow is represented by a complex potential function of hydrodynamics, and the velocity of the flow is obtained by differentiating the potential. When a mobile robot utilizes the velocity vector of the flow for the guidance, it can be guided along the stream line.

We had already proposed an application of the hydrodynamic potential in path planning for a mobile robot to avoid the obstacles and to reach the goal [5]. Hydrodynamic potential is constructed by superposing potential of a sink, a source (Fig. 1) and a dipole (Fig. 2), which represented a goal, a standing obstacle and a moving obstacle, respectively. In solving hydrodynamic problems, the boundary condition must be satisfied simultaneously at any point on the boundary of the body. However, in path planning problems, boundary condition should be satisfied only on the boundary of the robot body. That is, the volume of the computation with the complex potential function is very small, therefore, a mobile robot can avoid even moving obstacles. In addition, a mobile robot can move by switching the other flow of next calculation in real time in every cases even if it cannot achieve the planned flow.

In our previous research [5], a mobile robot can avoid the plural obstacles by using the superposition of the weighted flow fields where the largest weight is allotted to the flow generated by the nearest obstacle. A mobile robot can avoid the boundary of passage by introducing virtual obstacles synchronized with the movement of the robot along the boundary. A mobile robot can avoid the the obstacles even when the robot is trapped in a bottleneck narrower than the diameter of the mobile robot by using the vortex flow fields.

In this theory, there are two problems. One is that a mobile robot accelerates rapidly when it avoids the moving obstacle. The other is that a mobile robot has a discontinuous velocity when it is passing the moving obstacle. Therefore,

Seiji Sugiyama, Jyun Yamada and Tsuneo Yoshikawa are with College of Information Science and Engineering, Ritsumeikan University, Kusatsu, Shiga 525-8577, Japan, {seijisan@is, ci016060@ed, yoshikawa @ci}.ritsumei.ac.jp

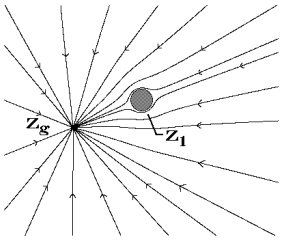

Fig. 1. The Flow Field $G_1(z)$ with the Standing Obstacle Z_1 and the Goal Z_g

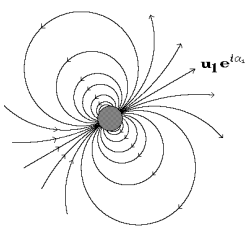

Fig. 2. The Flow Field $D_1(z)$ with the Moving Obstacle

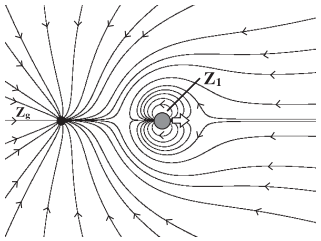

Fig. 3. The Flow Field by Using $\mathbf{G}_j(z) + \mathbf{D}_j(z)$

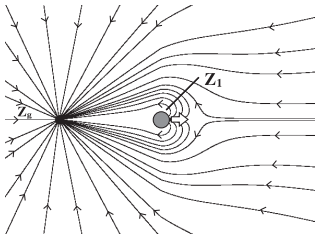

Fig. 4. The Flow Field by Using $\mathbf{G}_j(z) + \mathbf{D}_j(z)$ with $b_j(z)$

we propose a new improved velocity potential approach of hydrodynamic potential in this research. An ellipse field, which is obtained by using the conformal transformation, and a correction function, which generates the continuous velocity field, are installed in the previous potential function to cope with the difficulty.

In this paper, first, our previous theory of the hydrodynamic potential is described. Second, the ellipse field is introduced. Third, the correction function is utilized. Finally, simulations and the effectiveness of our research are shown.

II. Our Previous Hydrodynamic Potential

We assume that the dynamics of the mobile robot are governed by a first order delay system. This means that any control command to the robot will be realized in the control system with the delay time that is nearly equal to the time constant T. To cope with the delay time, the diameter of an avoidance circle for an obstacle is increased by the distance where the obstacle moves during the period T. The assumption leads us to focus the guidance of the robot on the path planning. We had applied the hydrodynamic potential successfully to the path planning [5]. Refer to the paper [6] for the details of the potential .

The complex flow potential $\mathbf{G}_j(z)$ in the complex plane z which has resulted from both a sink m at z_g and a cylinder a_j at z_j is represented by the following equation: (Fig. 1)

$$\mathbf{G}_j(z) = -m\log(z - z_g)(z - \tilde{z}_j) + m\log(z - z_j) \quad (1)$$

where $\tilde{z}_j$ denotes a point which is the mirror image with circle z_g, satisfying $(z_g - z_j)(\bar{\tilde{z}}_j - \bar{z}_j) = a_j^2$ ($\bar{z}_j$ is the complex conjugate of z_j). The dynamic of the flow in the shallow vessel suggests that the goal in the robotics field can be represented by a sink in the flow field and the obstacle by a cylinder whether it moves or not.

When an obstacle is moving with a velocity $u_j e^{i\alpha_j}$, the flow is described by a doublet as follows: (Fig. 2)

$$\mathbf{D}_j(z) = -\frac{a_j^2 u_j e^{i\alpha_j}}{z - z_j} \quad (2)$$

The total navigation function, including a single standing obstacle and a moving obstacle, is constructed by $\mathbf{G}_j(z)$ and $\mathbf{D}_j(z)$. Generally, a complex conjugate velocity for hydrodynamic potential $\mathbf{F}$ is obtained by $\bar{\mathbf{v}} = d\mathbf{F}(z)/dz$. That is, the guiding velocity of the robot is obtained by differentiating the composed potential both Eq. (1) and Eq. (2) and this flow field is shown in Fig. 3.

As the flow velocity becomes infinite at a sink according to its singularity, the function $\mathbf{G}_j(z)$ is correction by the following function $h(z)$ so that the navigation velocity may be limited to finite value.

$$h(z) = (1 - e^{-c_1|z - z_{st}|} + \epsilon)|z - z_g|(1 - e^{-c_2|z - z_g|}) \quad (3)$$

where z_{st} denotes start point, ϵ does a coefficient controlling the velocity at the start point, $\epsilon > 0$. c_1 is a coefficient controlling the acceleration at the start point, c_2 is a coefficient controlling the deceleration at the goal.

The doublet expressed by Eq. (2) generates attracting flow in the back side while it does repelling flow in the front side. This means that the robot will chase after an obstacle immediately after passing by it. Correction function $b_j(z)$ is introduced for correcting $\mathbf{D}_j(z)$ to assure the robot avoids and does not chase after the obstacle as shown below,

$$b_j(z) = \begin{cases} 1, & \text{for } \alpha_j - \frac{\pi}{2} \le \angle(z - z_j) \le \alpha_j + \frac{\pi}{2} \\ 0, & \text{for other} \end{cases} \quad (4)$$

where α_j denotes direction of the obstacle movement.

The path to avoid an obstacle j and to reach the goal is denoted by the velocity $\bar{\mathbf{v}_j}$ as shown in the following: (Fig. 4)

$$\bar{\mathbf{v}_j}(z) = h(z)\mathbf{G}_j^{'}(z) + b_j(z)\mathbf{D}_j^{'}(z) \quad (5)$$

where $'$ denotes differentiating operation by z. The equations for plural obstacles are omitted in this paper (Refer to [5]).

III. Flow Field by using Ellipse

Each of Figs. 5(a)–(d) shows the flow field by changing only one of the parameters of Fig. 3 respectively. Fig. 5(a) shows it by half m instead of Fig. 3. Similarly, Fig. 5(b) shows it by two times m. Fig. 5(c) shows it by half u_j, and Fig. 5(d) shows it by two times u_j. The increase of m or the decrease of u_j reduce the chasing area. However, there are two problems for set of m or u_j as follows.

One is that a standard velocity of a mobile robot without avoiding obstacles is set by using the constant value m. If m is larger, the velocity of a mobile robot is larger. And a mobile robot cannot move at a velocity that is faster than the maximum velocity of the robot. Therefore, it is difficult to change the value of m for only to reduce the chasing area.

The other is that u_j is set by using a velocity of a moving obstacle. That is, a mobile robot cannot set u_j. And u_j is always changed. Thus, a mobile robot rushes according to the value of u_j though it can avoid the arbitrarily moving obstacle in real time. So, it is necessary to make a velocity

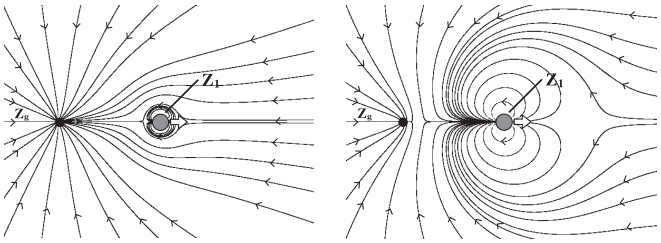

(a) Using half m (b) Using two times m

(c) Using half u_j (d) Using two times u_j

Fig. 5. Comparison of the Flow Fields by Using $G_j(z) + D_j(z)$

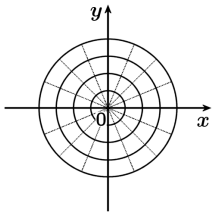

Fig. 6. z-plane

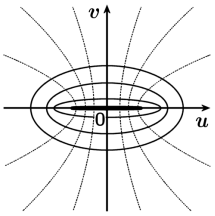

Fig. 7. w-plane

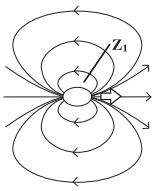

Fig. 8. The Flow Field around Ellipse

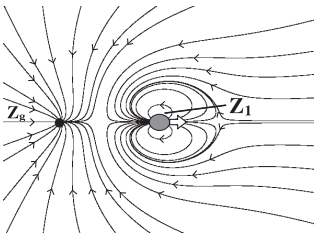

Fig. 9. The Ellipse Flow Field by using $\mathbf{G}_j(z) + \mathbf{D}_j(z)$

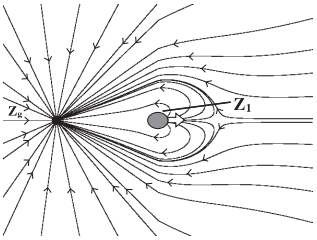

Fig. 10. The Ellipse Flow Field by using $\mathbf{G}_j(z) + \mathbf{D}_j(z)$ with $b_j(z)$

of a mobile robot slow for making use of a real robot. To get an appropriate velocity, a mobile robot avoids gradually when the moving obstacle is found in the further away. That is, an ellipse flow field mapped from an avoidance circle of a moving obstacle is used. The major axis of the ellipse is set to the direction of the moving obstacle α_j.

A. Conformal Transformation

It is assumed that the following equation denotes the relation of the complex numbers between $z = x+iy\,(z \in A)$ and $w = u + iv\,(w \in S)$.

$$w = f(z) \tag{6}$$

If the point z in A is made to correspond to the point w in S by $f(z)$, it is called a map (transformation) from A (z-plane) to S (w-plane). If two arbitrarily vectors in A are mapped attended with the same expansion and contraction and the rotation, it is called the "Conformal Transformation (CT)". If using CT, a minute area in the z-plane is mapped to the w-plane with the similar figure kept (the angle kept).

B. Zhukovsky Transformation

The following equation is called the "Zhukovsky Transformation (ZT)" for corresponding Eq. (6).

$$w = z + \frac{d^2}{z}; \quad (d > 0) \tag{7}$$

This is a method of mapping a circle to an ellipse in the CT. If Eq. (7) is differentiated, then

$$\frac{dw}{dz} = 1 - \frac{d^2}{z^2} \tag{8}$$

Therefore, Eq. (7) is a continuous function excluding $z = 0$. That is, the mapping $z \longleftrightarrow w$ of Eq. (7) denotes the CT.

If an arbitrarily point in the z-plane is represented by $z = re^{i\theta}$, and its corresponding point in the w-plane is represented by $w = u + iv$, then

$$u + iv = re^{i\theta} + \frac{d^2}{r}e^{-i\theta} \tag{9}$$

Therefore,

$$u = \left(r + \frac{d^2}{r}\right)\cos\theta, \quad v = \left(r - \frac{d^2}{r}\right)\sin\theta \tag{10}$$

1) Mapping to the Segment: If $r = d$, then Eq. (10) can be transformed as shown in the following: (Fig. 6 and Fig. 7)

$$u = 2d\cos\theta, \quad v = 0 \tag{11}$$

In Eq. (11), the corresponding point w rounds on the segment with $-2d$ and $2d$ at both ends when a point z rounds from $\theta = 0$ to 2π on the circumference of d in the radius in the z-plane. That is, a circle of d in radius in the z-plane can be mapped to the segment of $4d$ in length in the w-plane.

2) Mapping to the Ellipse: If $r > d$, then Eq. (10) can be transformed by eliminating θ as shown in the following:

$$\frac{u^2}{\left(r + \frac{d^2}{r}\right)^2} + \frac{v^2}{\left(r - \frac{d^2}{r}\right)^2} = 1 \tag{12}$$

This is the equation of the ellipse of which the center is on the origin, the major axis is represented by $(r + \frac{d^2}{r})$ and the minor axis is represented by $(r - \frac{d^2}{r})$.

3) Mapping to the Hyperbola: If $r < d$, then Eq. (10) can be transformed by eliminating r as shown in the following:

$$\frac{u^2}{(\sqrt{2}d\cos\theta)^2} - \frac{v^2}{(\sqrt{2}d\sin\theta)^2} = 1 \tag{13}$$

This is the equation of the hyperbola of which two focuses are $(2d, 0)$ and $(-2d, 0)$. The circle can be mapped not only to the ellipse, but also the surroundings of the ellipse to the corresponding points respectively as shown in Fig. 7.

C. Using the Conformal Transformation

To map the circle, that denotes the moving obstacle, to the ellipse is that ZT is applied to Eq. (2). That is,

$$D_j(z) = \left(r + \frac{d^2}{r}\right)\cos\alpha + i\left(r - \frac{d^2}{r}\right)\sin\alpha \tag{14}$$

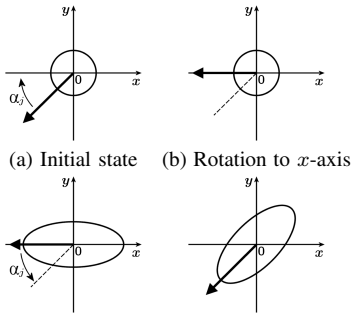

(a) Initial state (b) Rotation to x-axis

(c) Mapping to the Ellipse field (d) Returning to the first angle

Fig. 11. Rotation of Ellipse

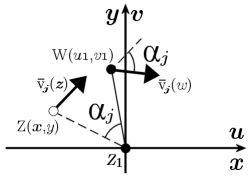

Fig. 12. The Relation Between z-plane and w-plane

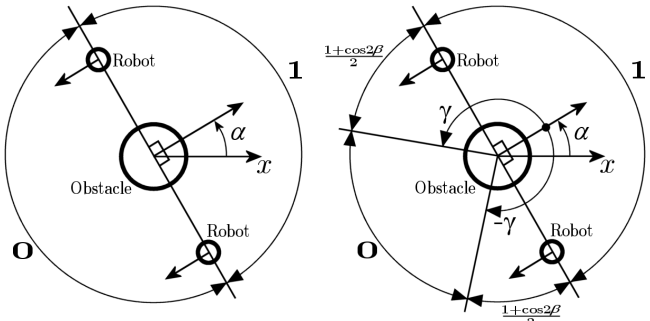

(a) Previous $b_j(z)$ (b) New $b_j(z)$

Fig. 13. Arrangement of areas in $b_j(z)$

Fig. 8 shows the flow field of the ellipse doublet. Fig. 9 shows the flow field $\mathbf{G}_j(z)+\mathbf{D}_j(z)$ with the ellipse. Fig. 10 shows the flow field $\mathbf{G}_j(z) + \mathbf{D}_j(z)$ with the ellipse and $b_j(z)$. If using the ellipse doublet, it can be found that the flow field around the moving obstacle becomes wider than the previous flow field (Compare Fig. 3 and Fig. 9, Fig. 4 and Fig. 10). Therefore, a mobile robot can gradually avoid a moving obstacle from further away by using the ellipse.

D. Rotation of Ellipse

If using Eq. (14), the direction of the major axis is only on the direction of x-axis. Therefore, the rotation matrix is used for mapping the direction of the moving obstacle to the direction of the ellipse.

We assume that w denotes the corresponding point of which the point Z in the z-plane rotates α_j. And its rotation matrix is represented by R_1 as the following:

$$W = R_1 Z; \quad R_1 = \begin{bmatrix} \cos\alpha_j & \sin\alpha_j \\ \sin\alpha_j & -\cos\alpha_j \end{bmatrix} \tag{15}$$

Figs. 11(a)–(d) show the sequence of the transformations for rotating the ellipse. First, Fig. 11(a) shows the obstacle with progressing the direction to the left-down, and its flow field is represented by Eq. (5). Second, Fig. 11(b) shows the starting to rotate for x-axis with the mapping into the ellipse, and its equation is represented by the following:

$$\bar{\mathbf{v}_j}(w) = R_1 \left(h(z)\mathbf{G}_j^{'}(z) + b_j(z)\mathbf{D}_j^{'}(z) \right) \tag{16}$$

Third, the corresponding point w and the velocity $\bar{\mathbf{v}_j}(w)$ in the w-plane can be satisfied the relation between the point z and the velocity $\bar{\mathbf{v}_j}(z)$ in the z-plane by using Eq. (16) as shown in Fig. 12. This transformation is shown in Fig. 11(c), and Eq. (14) is substituted in Eq. (16) as the following:

$$\bar{\mathbf{v}_j}(w) = R_1 \left(h(w)\mathbf{G}_j^{'}(w) + b_j(w) \left(\mathbf{D}_j^{'}(w) + \frac{(du_j)^2}{\mathbf{D}_j^{'}(w)} \right) \right) \tag{17}$$

Finally, the rotation matrix for returning to the first angle is represented by the following:

$$R_2 = \begin{bmatrix} \cos(-\alpha_j) & \sin(-\alpha_j) \\ \sin(-\alpha_j) & -\cos(-\alpha_j) \end{bmatrix} \tag{18}$$

And it becomes the following: (Fig. 11(d))

$$\bar{\mathbf{v}_j}(w) = R \left(h(w)\mathbf{G}_j^{'}(w) + b_j(w) \left(\mathbf{D}_j^{'}(w) + \frac{(du_j)^2}{\mathbf{D}_j^{'}(w)} \right) \right) \tag{19}$$

where R denotes the combining $R_2 R_1$ as the following:

$$R = R_2 R_1 = \begin{bmatrix} \cos 2\alpha_j & \sin 2\alpha_j \\ -\sin 2\alpha_j & -\cos 2\alpha_j \end{bmatrix} \tag{20}$$

The differences between Eq. (19) and Eq. (5) are just R and $(du_j)^2/\mathbf{D}_j^{'}(w)$. Especially, the size of the ellipse is generated by corresponding $(du_j)^2$. This parameter is included in the velocity of a moving obstacle u_j, so a mobile robot can gradually avoid from an early stage according to the velocity of the moving obstacle .

IV. Improvement of Correction Function

In the previous equations [5], the correction function $b_j(z)$ is not continuous. This means that the velocity of the mobile robot is changed rapidly at a discontinuous point, because $b_j(z)$ have only two values: 0 and 1. So, it is necessary to define the new $b_j(z)$ for set a continuous function.

The role of $b_j(z)$ is to avoid the chasing a moving obstacle immediately after passing by it. If adjusting the relation between a sink m and a velocity u_j, the chasing motion of the moving obstacle can be avoided as shown in Figs. 5(a)–(d). However, the velocity of a moving obstacle is not continuous and is irregular in real environment. If m changes frequently up and down according to the changing u_j, the velocity of a mobile robot changes too frequently though the motion of chasing the moving obstacle does not occur. Therefore, it is necessary for the method of using no changing the value of m to avoid the chasing motion. That is, $b_j(z)$ is a necessity function.

Fig. 13(a) shows the arrangement of areas of 1 and 0 by using the previous $b_j(z)$. These two values of 1 and 0 are changed on the point where the angle between the direction of the mobile robot and the direction of the obstacle is $\frac{\pi}{2}$. So, $D_j(z)$ is neglected immediately when the moving obstacle has passed. To solve this problem, the following new $b_j(z)$ is

redefined instead of the previous $b_j(z)$ as shown in Eq. (4).

$$b_j(z) = \begin{cases} 1, & \text{for } \alpha_j - \frac{\pi}{2} \le \angle(z - z_j) \le \alpha_j + \frac{\pi}{2} \\ \dfrac{1 + \cos 2\beta_j}{2}, & \text{for } \alpha_j + \frac{\pi}{2} < \angle(z - z_j) < \alpha_j + \gamma \\ & \text{or } \alpha_j - \gamma < \angle(z - z_j) < \alpha_j - \frac{\pi}{2} \\ 0, & \text{for other} \end{cases} \tag{21}$$

where α_j denotes the direction of the moving obstacle, γ denotes the terminal angle for using cosine function, β_j is represented by the following.

$$\beta_j = \angle(z - z_j) - \left(\alpha_j + \frac{\pi}{2}\right) \tag{22}$$

A cosine function is installed at the discontinuous point, so $b_j(z)$ is changed smoothly from 1 to 0 in Eq. (21). Fig. 13(a) shows the arrangement of areas of 1 and 0 by using the previous $b_j(z)$. Fig. 13(b) shows the arrangement of areas of 1, $(1 + \cos 2\beta_j)/2$ and 0 by using the new $b_j(z)$.

Figs. 14(a)–(d) show the flow fields by using the new correction function $b_j(z)$, where Figs. 14(a),(b) use $\gamma = \pi$ and Figs. 14(c),(d) use $\gamma = \frac{3\pi}{4}$. The overshooting paths, that is chasing curve to the moving obstacle, by using $\gamma = \frac{3\pi}{4}$ are smaller than the overshooting paths by using $\gamma = \pi$. Therefore, we decide to use $\gamma = \frac{3\pi}{4}$ in the simulation of the next chapter.

Compare Figs. 14(a),(c) and Fig. 4 by using the circle. And also compare Figs. 14(b),(d) and Fig. 10 by using the ellipse. It can be found that the discontinuous points are appeared as shown in Fig. 4 and Fig. 10. However, no discontinuous point is appeared as shown in Figs. 14(a)–(d). That is, it can be shown that the new correction function $b_j(z)$ has no discontinuous point and no chasing the moving obstacle. Moreover, it can be found that the flow field by using ellipse is wider than the flow field by using circle. That is, using an avoidance ellipse is more safety than using avoidance circle. Therefore, hereinafter, we decide to use the style of Fig. 14(d) for avoiding the moving obstacle.

V. Simulation

The flow field to the preceding chapter is drawn without actual move of the obstacle. The reason is that the characteristic of the flow field with the moving obstacle cannot be displayed simply. However, the moving obstacle will move itself in the real environment. Therefore, we investigate the usefulness of the new method in the simulation.

A. Our Previous Method

Fig. 15 shows our previous simulation by using Hydrodynamic Potential where a mobile robot avoids one moving obstacle and can reach the goal. In this figure, many circles display the location of both the mobile robot and the moving obstacle respectively at the constant interval. Before the start of the simulation, the obstacle stands the right side, and the mobile robot stands the left side in the simulation display area. Moreover, the goal is set at the right side. The moving obstacle moves to the left direction and the mobile robot moves to the right direction after starting this simulation. If

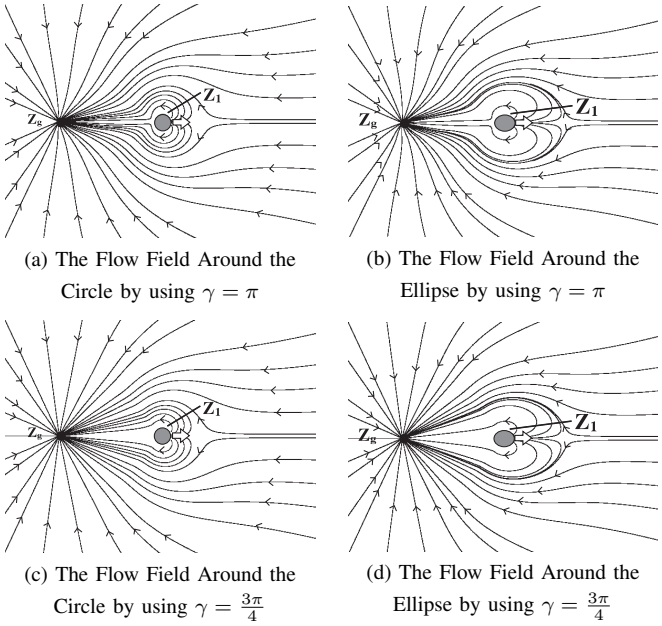

(a) The Flow Field Around the Circle by using $\gamma = \pi$

(b) The Flow Field Around the Ellipse by using $\gamma = \pi$

(c) The Flow Field Around the Circle by using $\gamma = \frac{3\pi}{4}$

(d) The Flow Field Around the Ellipse by using $\gamma = \frac{3\pi}{4}$

Fig. 14. The Flow Fields by using New $b_j(z)$

the distance between two circles is long, it is shown that the velocity is fast. In the intersection on near the center of display area, it can be seen that the mobile robot can avoid the moving obstacle. However, the velocity of the mobile robot accelerates rapidly when it avoids a moving obstacle.

B. New Method by using Conformal Transformation

Fig. 16 shows the simulation with the new method by using CT. That is, the ellipse flow field is used in this simulation. The initial conditions of Fig. 16 is the same as those of Fig. 15. In comparison of Fig. 15, Fig. 16 and Fig. 17, the difference of their velocities is shown. It can be seen that the maximum velocity of the new method is a half maximum velocity of our previous method. As a result, the effectiveness of our method by using the ellipse flow field can be shown.

C. New Method with Applying Correction Function

Fig. 18 shows the simulation with applying the correction function $b_j(z)$ in Fig. 15. And Fig. 19 shows the simulation with applying correction function $b_j(z)$ in Fig. 16. Similarity, Fig. 20 also shows the difference of their velocities. It can be seen that the case of Fig. 19 is smoother than the case of Fig. 18. The blue line as shown in Fig. 17 has a discontinuous point at the maximum velocity point. However, the blue line as shown in Fig. 20 has no discontinuous point at all time. As a result, the effectiveness of our method by using the new correction function can be shown.

D. Discussion

Is the robot motion considered? If the robot is just in front of the obstacle, how does the robot move? These answers are very simple. That is, the robot can move while touching the avoidance circle of the obstacle. If the obstacle does not move, the robot can always avoid the obstacle. If the

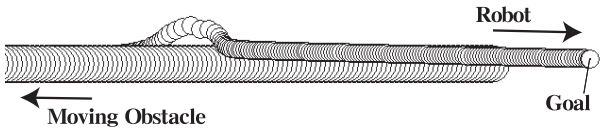

Fig. 15. The Flow Field by using the Previous Method

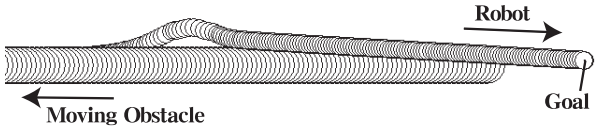

Fig. 16. The Flow Field by using the Conformal Transformation

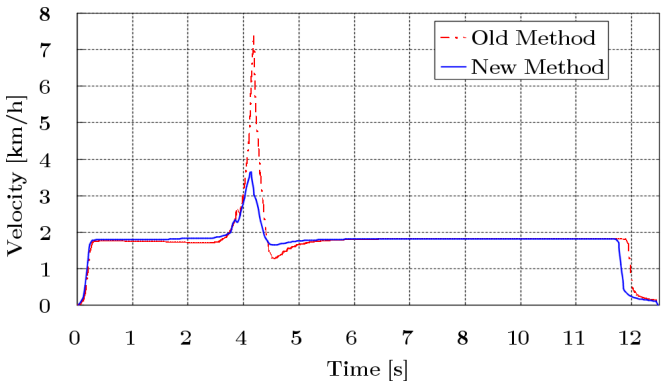

Fig. 17. The velocities of Fig. 15 and Fig. 16

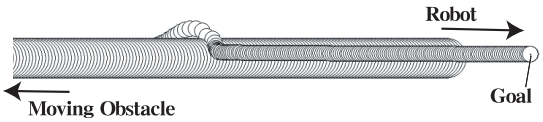

Fig. 18. The Flow Field of Fig. 15 with the new $b_j(z)$

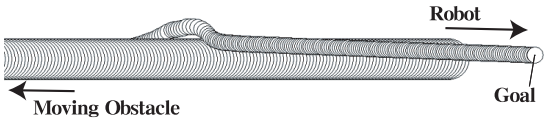

Fig. 19. The Flow Field of Fig. 16 with the new $b_j(z)$

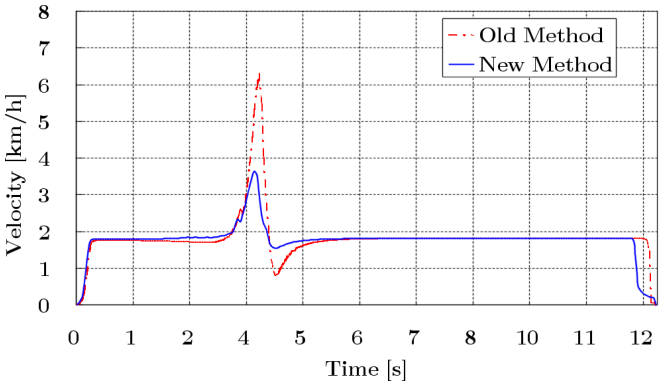

Fig. 20. The velocities of Fig. 18 and Fig. 19

obstacle moves, the robot can avoid the obstacle by using an increased diameter of an avoidance circle to cope with the delay time that is nearly equal to the time constant T. Therefore, the robot can always avoid the obstacle in real time. In this paper, we discuss that this increased velocity by the moving obstacle is reduced. That is, it is assumed that the robot can search the obstacle from further away. Generally, if the robot faces just in front of the moving obstacle that has a rapid velocity that is larger than the maximum velocity of the robot, the robot can not avoid the moving obstacle in any manner. If the obstacle is in further away and using the proposed method, the robot can avoid the moving obstacle without a rapid velocity. Note that the increased velocity faces the avoidance direction in our proposed method and this is safety if the robot can achieve the velocity and can search the obstacle from further away.

It might be seemed that it is questionable that Fig. 17 and Fig. 20 come from both the ellipse field and the correction function, and they are only influenced by the parameters of m and u_j. However, the m and the u_j are the same value, respectively in each simulation. The m denotes a sink value and the standard robot velocity comes from the m. That is, the m can not be changed. This can be seen by the vertical constant velocity lines shown in Fig. 17 and Fig. 20. On the other hand, the u_j denotes the obstacle velocity. That is, the u_j can not be changed too. All distances of many circles of the moving obstacles shown in both Fig. 15 and Fig. 16, and also both Fig. 18 and Fig. 19 are the same, respectively. Therefore, the changing velocities of these simulations come from the other factors. The factors are using both the ellipse field and the correction function.

VI. Conclusion

In this paper, we proposed the improved method by applying the Conformal Transformation and the new correction function to our previous Hydrodynamic Potential method for path planning of a mobile robot to avoid the moving obstacle smoothly. A mobile robot can gradually avoid a moving obstacle from further away, and can be safely guided without rapid acceleration. And the new correction function has no discontinuous velocity. So, a mobile robot can pass a moving obstacle smoothly. If a mobile robot avoids the arbitrarily moving obstacle with quick changing of velocity at the near of the obstacle, the guidance velocity becomes large. However, if using our new method, the velocity variation of the robot can be reduced. We will construct an experiment on a real mobile robot by using the new method and will investigate the usefulness of our research in the future.

References

[1] S. Akishita, S. Kawamura and K.Hayashi, “New Navigation Function Utilizing Hydrodynamic Potential for Mobile Robot”, Proc. of the 1990 IEEE international Workshop on Intelligent Motion Control, Catalog Number: 90 TH0272-5, pp. 413–417, 1990

[2] S. Akishita, S. Kawamura and T. Hisanobu, “Velocity Potential Approach for Path Planning to Avoid Moving Obstacles”, J.of Advanced Robotics, Vol.7, No.5, pp.463-478, 1993

[3] O. Khatib, “Real-time obstacle avoidance for manipulators and mobile robots”, Int. J. for Robotics Research, 5(1), pp. 90–98, 1986

[4] P. Khosla and R. Volpe, “Super quadric potential for obstacle avoidance and approach”, IEEE Conf. on Robotics and Automation, pp. 1778–1784, 1988

[5] S. Sugiyama and S. Akishita, “Path Planning for Mobile Robot at A Crossroads by Using Hydrodynamic Potential”, Proceedings of 1998 JAPAN-U.S.A SYMPOSIUM ON FLEXIBLE AUTOMATION, pp. 595–602, 1998

[6] H. LAMB, “HYDRODYNAMICS”, Cambridge University Press Sixth Editions, 1975